Data Fusion: Applying Chemometric Modeling to Gamma and Optical Spectroscopic Data

Prepared for
US Department of Energy

Shirmir D. Branch, Heather M. Felmy, Dana L. Arbova, Grey Batie, Erin C. Good, Samuel A. Bryan, Amanda M. Lines

Pacific Northwest National Laboratory

May 2025
PNNL- 37731

DISCLAIMER

PACIFIC NORTHWEST NATIONAL LABORATORY
operated by
BATTELLE
for the
UNITED STATES DEPARTMENT OF ENERGY
under Contract DE-AC05-76RL01830

Printed in the United States of America

Available to DOE and DOE contractors from
the Office of Scientific and Technical Information,
P.O. Box 62, Oak Ridge, TN 37831-0062
www.osti.gov
ph: (865) 576-8401
fox: (865) 576-5728
email: reports@osti.gov

Available to the public from the National Technical Information Service
5301 Shawnee Rd., Alexandria, VA 22312
ph: (800) 553-NTIS (6847)
or (703) 605-6000
email: info@ntis.gov
Online ordering: http://www.ntis.gov

Data Fusion: Applying Chemometric Modeling to Gamma and Optical Spectroscopic Data

May 2025

Shirmir D. Branch
Heather M. Felmy
Dana L. Arbova
Grey Batie
Erin C. Good
Samuel A. Bryan
Amanda M. Lines

Prepared for
the U.S. Department of Energy
under Contract DE AC05 76RL01830

Pacific Northwest National Laboratory
Richland, Washington 99354

SUMMARY

Molten salt reactors are a promising Gen IV design that could potentially supply safe, efficient, and green energy. However, methods for completing material control and accounting could still be optimized for effective utilization and support of these systems. Radiometric data can provide highly valuable insight into the isotopic composition of molten salts. Optical techniques, such as UV-vis and Raman, can provide elemental and speciation composition of molten salts. The combination of these two approaches through data fusion can 1) provide more comprehensive characterization of a given chemical system and 2) potentially provide a pathway to reduce uncertainty of measurements. This can be particularly valuable in molten salt reactor (MSR) salt loops where batches are expected to be highly complex in composition which will produce complex data derived from any analytical technique. Advanced data analysis will be needed for accurate interpretation of the data obtained from MSR reactor fuels. Furthermore, tools that can automate analysis or allow analysis to occur in real-time or near real-time would be game-changing for on-line monitoring approaches, especially when using multiple techniques to inform the same system.

Here, the application of chemometric modeling to multiple sets of spectroscopic data is explored to outline possible routes for highly accurate and automated sensor fusion data analysis. Chemometric modeling is a form of chemical data science that has been extensively applied to data streams including optical spectroscopy data and as a proof of concept for gamma spectroscopic data. It utilizes a multivariate approach to characterize and quantify chemical targets. Each of these techniques provides different information that more thoroughly informs accountancy on a single chemical system. This is demonstrated by building chemometric models based on Raman, UV-vis, and gamma data of a single chemical system and fusing that sensor data to build a single model. The resulting models show good accountancy of a target species when sensor data is fused as compared to models relying on only one instrument source for data. The results are promising and suggest further investigation into more complex chemical systems which can include a multi-analyte aqueous system or a proof-of-concept demonstration on a molten salt sample.

This report meets milestone M3RS-25PN0401042, “Data fusion of optical and gamma spectroscopy for chemometric analysis”.

CONTENTS

FIGURES

TABLES

ACRONYMS AND ABBREVIATIONS

DOE	US Department of Energy
DSA	digital signal analyzer
FY	fiscal year
MC&A	material control & accountancy
MCA	multi-channel analyzer
MSC	multiplicative scatter correction
MSR	molten salt reactor
NIST	National Institute of Standards and Technology
PC	principal component
PCA	principal component analysis
PCR	principal component regression
PNNL	Pacific Northwest National Laboratory
RMSEC	root-mean-square error of calibration
RMSECV	root-mean-square error of cross validation
UV-vis	Ultraviolet-visible

1. Introduction

Next generation nuclear reactor designs offer safety and performance improvements compared to the existing and operating reactors. Molten salt reactors (MSRs) are an example of this, providing improved energy harvesting efficiency and very low likelihood of uncontrolled criticality. However, MSRs represent a paradigm shift, and new tools will be needed to support a variety of needs, including meeting material control and accounting (MC&A) requirements. Monitoring via a wide variety of tools and sensors can meet these needs, provided tools are advanced to perform within the conditions anticipated for MSR systems.

Radiometric monitoring, for example is important to safeguarding fuel within an MSR.[1] Spectroscopic monitoring is also useful to inform MSR chemistry and elemental composition both at the front and back end of MSR operations.[2, 3] These and other analytical techniques proposed for the MC&A of MSRs are anticipated to have significant signal complexity. This complexity of signal would make it difficult to accurately and quickly analyze radiometric data using existing approaches to analyzing such data. The use of advanced chemometric methods has been demonstrated for gamma spectral data of aqueous reprocessing solutions under aqueous reprocessing conditions[4-6], as well as optical spectral data of a molten chloride system.[7]

This report aims to build on previous work to develop quantitative chemometric modelling approaches using both gamma and optical spectroscopic techniques. Models were developed on both uranium and plutonium spectral data and analyzed using principal component regression (PCR). Comparisons are made between models developed using a single technique (gamma, ultraviolet-visible (UV-vis), or Raman) and models made fusing the data from all techniques into a single model. Chemometric modeling has been extensively applied to a wide range of data types to enable highly accurate data analysis.[8-13] However, it has not yet been applied to any large extent to gamma spectroscopy data, though some machine learning demonstrations have been completed.[14] Data fusion methods can allow for more robust models, where spectral fingerprint information can be provided by multiple techniques.[15, 16] These fused models can also be applied to more systems where a single technique would be insufficient to quantify all analytes of interest. Another key opportunity to be explored is the ability of data fusion models to lower uncertainty of quantification through the combination of disparate data streams. This will be addressed as proof of concept here, where initial positive results suggest further study in the future could be valuable.

2. SETUP AND METHODOLOGIES

2.1. Sample Preparation

Samples of uranyl nitrate, $UO_2(NO_3)_2$ or plutonium (IV) nitrate, $Pu(NO_3)_4$ in a nitric acid matrix were analyzed according to the concentrations listed in Table 2-1. The samples were prepared from the stock concentration received. Sample dilutions were chosen to match concentration ranges expected in a typical solvent extraction system. UV-vis and

Raman samples were collected first. Those same samples were then counted at the gamma detector.

Table 2-1. Concentrations of U sample series and Pu sample series used in in this study.

$[UO_2^{2+}]$, M in 0.27 M HNO_3	$[Pu^{4+}]$, $\times 10^{-3}$ M in 0.5 M HNO_3
1.96	32.76
0.98	9.90
0.49	4.95
0.25	2.47
0.12	1.24
0	0.62
	0.31
	0.15
	0.08
	0

2.2. Instrumentation

Raman and UV-Vis spectroscopic instruments were acquired from Spectra Solutions Inc., and each utilized a high throughput volume phase holographic grating spectrograph with a thermoelectrically cooled two-dimensional charge-coupled device detector. The UV-vis instrument had a functional wavelength range of approximately 450 – 850 nm. The Raman instrument utilized a ~200 mW 532 nm excitation laser with a fiber optic Raman probe with a backscattering (180°) optical design. The wavenumber axis was calibrated using naphthalene and the resolution was <5 cm^{-1}. The wavenumber range was 140 – 4500 cm^{-1}.

Gamma spectroscopy measurements were systematically conducted using low-energy germanium detectors (LEGes) with thin beryllium windows, optimized for performance in the energy range of 46 to 1000 keV. The Lynx digital signal analyzer (DSA) module from Mirion Technologies (Meriden, CT, USA) was employed to process the signals from the detectors. The Lynx module utilizes an ultra-fast Analog-to-Digital converter to digitize the signals, which are then stored in an integrated multi-channel analyzer (MCA). The Genie2000 Spectroscopy Software Suite, developed by Mirion Technologies, was used to perform the analysis, including isotopic identification and quantification. The detectors were energy and efficiency calibrated using standards traceable to the National Institute of Standards and Technology (NIST).

2.3. Chemometric Modeling

Gamma and optical spectral processing were performed using MATLAB Version 9.13 (R2022b),[17] and chemometric modeling was performed using PLS Toolbox Version 9.2.1 software from Eigenvector Research Inc.[18] PCR[19] models were developed for the quantification of U and Pu using gamma, UV-vis, and Raman spectral data. Details on the use of chemometric modeling for spectral data are discussed elsewhere.[8] The gamma data was first normalized by dividing the counts at each energy by the total number of

counts in the spectrum. This data was then preprocessed by applying a multiplicative scatter correction (MSC) following by mean centering the data. The UV-vis data was preprocessed by applying a first derivative (second-order polynomial with a 15-point filter width) followed by mean centering. The Raman data was preprocessed by first applying a first order baseline correction to the water band (2500 – 4000 cm^{-1}) followed by a normalization to the area under the water band to account for fluctuations in the laser power over time. A first derivative (second-order polynomial with a 15-point filter width) was then applied followed by mean centering. 3 principal components (PCs) were used for the U models and 4 PCs were used for the Pu models. For fused models, spectral data from gamma, UV-vis, and Raman were individually preprocessed and then fused into a single dataset using the Multiblock Model tool in PLS Toolbox. A block variance scaling was applied to each set of data to account for differences in signal intensity between techniques. A “leave one out” cross validation method was utilized where one sample was successively removed from the model and then the remaining samples were used to predict the concentration of the removed sample. This was repeated until every sample was left out of the model. This was used as a validation of model performance. This cross validation method was employed due to the small dataset.

3. RESULTS AND DISCUSSION

3.1. Discussion of raw data

The U spectral data collected to build the regression models below are shown in Figure 3-1. The spectra were collected as a series of 2-fold dilutions from 1.96 M to 0.1225 M plus a 0 M as a blank. Figure 3-1A shows the gamma spectra of these samples, with the inset showing characteristic peaks that include signatures at 92.78 and 186.20 keV, which are consistent with U-238[20] and U-235,[21] respectively. The UV-vis data in Figure 3-1B shows an optical fingerprint at ~485 nm and below[22]. The Raman data in Figure 3-1C shows fingerprints at ~870 cm^{-1} and ~1050 cm^{-1} for UO_2^{2+} [22] and NO_3^-,[23] respectively. All of these unique signatures showed the anticipated decrease in spectral response as the concentrations were diluted 2-fold.

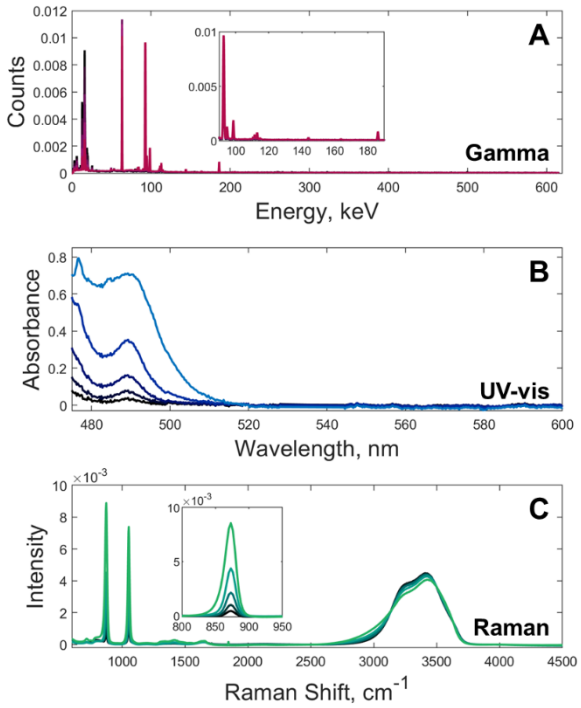

Figure 3-1. Spectra of U at various concentrations in 0.27 M HNO_3: (A) Gamma spectra with inset showing gamma signatures for U-235 and U-238; (B) UV-vis spectra of showing absorbance signature for UO_2^{2+}; and (C) Raman spectra with inset showing Raman signature for UO_2^{2+}.

The Pu spectra showed similar trends based on dilution as shown in Figure 3-2. The gamma spectrum in Figure 3-2A includes characteristic peaks at 43.5 keV for Pu-238, 45.23 keV for Pu-240, and 51.63 keV for Pu-239.[24] The absorbance spectra show Pu^{4+} peaks at around 480 nm, 550 nm, 660 nm, and 805 nm (Figure 3-2B).[25] Pu^{4+} does not have any Raman active signatures (Figure 3-2C) because Raman is a vibrational technique and captures molecular species. Therefore, an individual Raman PCR model was not built.

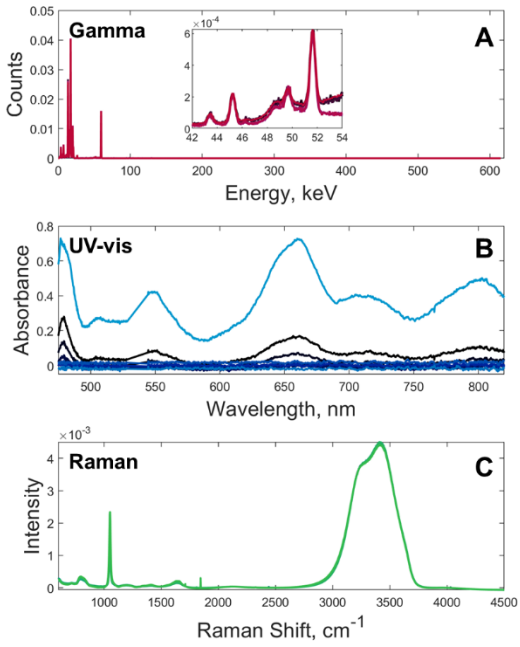

Figure 3-2. Spectra of Pu^{4+} at various concentrations in 0.5 M HNO_3: (A) Gamma spectra with inset showing gamma signatures for Pu-238, Pu-239, and Pu-240; (B) UV-vis spectra of showing absorbance signature for Pu^{4+}; and (C) Raman spectra with no Pu^{4+} signatures.

3.2. Chemometric modeling and regression

Individual PCR models were built for the quantification of UO_2^{2+} using gamma, UV-vis, and Raman techniques. The results are shown in Figure 3-3. These parity plots show the known UO_2^{2+} concentration vs. the model measured UO_2^{2+} concentration. The 1:1 slope of the regression indicates an accurate model. The model statistics are provided in Table 3-1. These include the root-mean-square error of calibration (RMSEC) which provides the uncertainty in the calibration data as well as the root-mean-square error of cross validation (RMSECV) which is the uncertainty of prediction for data left out of the model. The RMSECV values were larger than the RMSEC, which is expected when a sample is removed from the dataset and the model is built from the remaining samples. From Figure 3-3 and the RMSE values, it can be seen that Raman was the most accurate technique for the quantification of UO_2^{2+} in this concentration range and gamma was the least accurate of the three techniques.

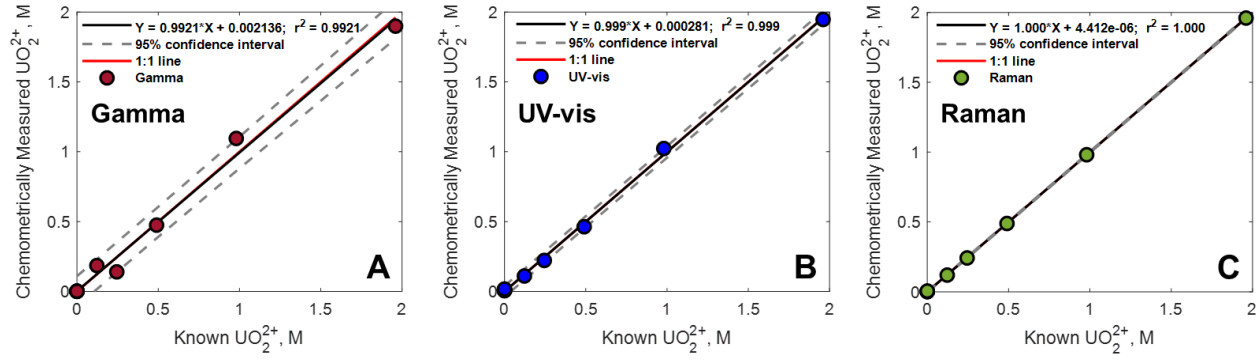

Figure 3-3. PCR regression analysis of UO_2^{2+}: (A) Gamma; (B) UV-vis; (C) Raman.

PCR models were also developed for the quantification of Pu^{4+} and the results are shown in Figure 3-4 and Table 3-1. In this case, UV-vis was the best technique for the quantification of Pu^{4+} shown by the lower RMSE values. For Pu^{4+}, Raman would be the worst technique as Pu^{4+} is Raman inactive and therefore, a model was not built. The RMSECV values are again higher than the RMSEC due to the relatively small sample set. The comparison of chemometric models of these two radionuclides is a good example of the importance of using multiple techniques simultaneously, in order to provide quantification of multiple species of interest, where a single technique alone would be insufficient.

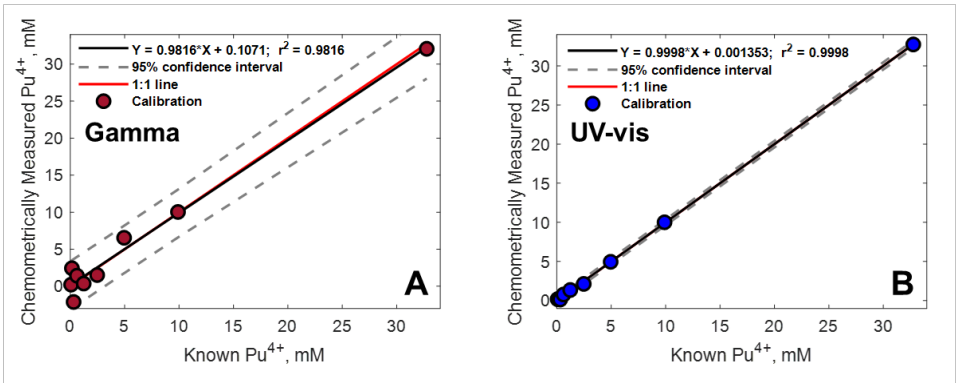

Figure 3-4. PCR regression analysis of Pu^{4+}: (A) Gamma; (B) UV-vis.

A comparison was then made between models built on individual techniques and fused data. Figure 3-5 shows a comparison of the model results for each individual technique (Figure 3-5A and Figure 3-5C) and the fused models with data from the three techniques combined into a single model for UO_2^{2+} (Figure 3-5B) and Pu^{4+} (Figure 3-5D). The model statistics for the fused models are also provided in Table 3-1. In the case of UO_2^{2+}, the fused model RMSEs were similar to the Raman dataset, indicating again that Raman is the preferred technique for the quantification of uranyl in the concentration range studied here. This may not be the case at different concentration ranges. The Pu fused model performed better than any individual model and was similar to the UV-vis model. This

work shows that combining data from multiple sources can improve the accuracy of quantification. But even in cases where uncertainty is not improved, the fused models performed similar to the best individual technique, meaning that accuracy is not lost. Plus, data fusion techniques can provide a simplified and more automated analysis and can be applied to more complex analyte streams where a single technique cannot be used for every analyte of interest.

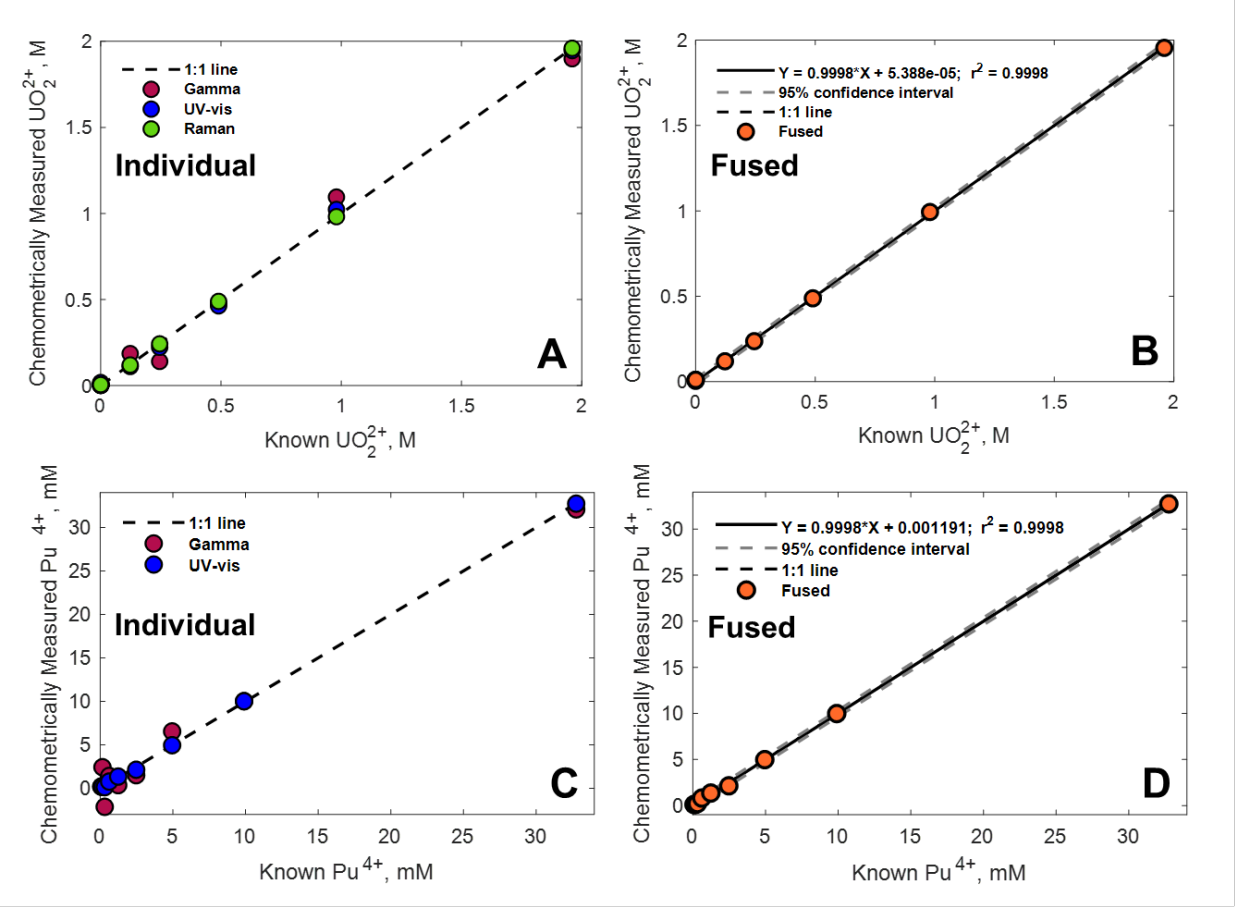

Figure 3-5. PCR regression analysis of UO_2^{2+} and Pu^{4+}: (A) overlay of individual models for UO_2^{2+}; (B) fused model for UO_2^{2+}; (C) overlay of individual models for Pu^{4+}; (D) fused model for Pu^{4+}.

Table 3-1. Model statistics including calibration uncertainty (RMSEC) and cross-validation uncertainty (RMSECV) for models built on gamma, UV-vis, and Raman individually as well as fused models of all three datasets.

	U		Pu	
Technique	RMSEC, M	RMSECV, M	RMSEC, $\times 10^{-3}$M	RMSECV, $\times 10^{-3}$M
Gamma	0.048	0.19	1.4	9.1
UV-vis	0.017	0.33	0.15	3.7
Raman	0.0022	0.016	N/A	N/A
Fused	0.0076	0.097	0.14	3.6

4. CONCLUSION AND RECOMMENDATIONS

In this work, it was demonstrated that data science tools such as chemometric modeling can be used in concert with data fusion, or the combination of data from multiple sensors, to build highly accurate and precise models for quantification of uranium and plutonium. In general, observed trends suggest models built from fused data can exhibit lower uncertainties than models built from data collected on a single sensor modality. This was demonstrated on uranyl and Pu(IV), where a series of samples were measured on Raman, UV-is, and gamma spectroscopy. In the uranyl system the fused model outperformed the UV-vis and gamma models in terms of lower uncertainties. Interestingly, the Raman model did display a lower uncertainty than the fused model, but this is likely due to the very strong Raman fingerprint displayed by uranyl. Similarly, for the Pu(IV) system, UV-vis and fused models showed relatively similar uncertainties. It should be noted this same performance may not be observed for other chemical targets or continue to persist in more complex mixed systems. In addition to potentially reducing error in quantification, the data fusion approach also provides the opportunity for multiple systems or analytes to be analyzed simultaneously, also allowing for a more complete picture of the MSR behavior and accounting.

Each analytical technique modeled in this work provides benefits for MC&A of MSR systems. It should be noted that the applicability of chemometric modeling is not limited to only these techniques. There is potential to incorporate other techniques – such as electrochemistry or other spectroscopies – into fused models to further inform the MC&A of MSRs and other systems while reducing uncertainty of quantification. Additionally, this fused model approach to accuratelyaccount for the species in these aqueous samples using multiple analytical techniques sets the groundwork for integrating into more complex chemical systems, such as the combined data fusion modelling on a molten salt sample.

5. ACKNOWLEDGMENTS

This work was funded by the Department of Energy Office of Nuclear Energy's Advanced Reactor Safeguards Campaign. Pacific Northwest National Laboratory (PNNL) is operated by Battelle Memorial Institute for the DOE under contract DE-AC05-76RL01830.

6. REFERENCES

(1) Dion, M. P.; Worrall, L. G.; Croft, S.; Scott, L. M. *Molten Salt Reactor Signatures and Modeling Study*; United States, 2021. https://www.osti.gov/biblio/1761616 https://www.osti.gov/servlets/purl/1761616DOI: 10.2172/1761616.
(2) Skutnik, S. E.; Sobel, P. W.; Swinney, M. W.; Hogue, K. K.; Arno, M. M.; Chirayath, S. S. Survey of prospective techniques for molten salt reactor feed monitoring. *Annals of Nuclear Energy* **2024**, *208*, 110796. DOI: 10.1016/j.anucene.2024.110796.
(3) Kirsanov, D.; Rudnitskaya, A.; Legin, A.; Babain, V. UV–Vis spectroscopy with chemometric data treatment: an option for on-line control in nuclear industry. *Journal of Radioanalytical and Nuclear Chemistry* **2017**, *312* (3), 461-470. DOI: 10.1007/s10967-017-5252-8.
(4) Coble, J.; Meier, D. Monitoring Aqueous Reprocessing Systems for Detection of Facility Misuse. *IEEE Transactions on Nuclear Science* **2019**, *66* (4), 729-736. DOI: 10.1109/TNS.2019.2900583.
(5) Orton, C. R.; Fraga, C. G.; Christensen, R. N.; Schwantes, J. M. Proof of concept simulations of the Multi-Isotope Process monitor: An online, nondestructive, near-real-time safeguards monitor for nuclear fuel reprocessing facilities. *Nuclear Instruments and Methods in Physics Research Section A: Accelerators, Spectrometers, Detectors and Associated Equipment* **2011**, *629* (1), 209-219. DOI: https://doi.org/10.1016/j.nima.2010.10.024.
(6) Schwantes, J. M.; Bryan, S. A.; Orton, C. R.; Levitskaia, T. G.; Pratt, S. H.; Fraga, C. G.; Coble, J. B. Advanced Process Monitoring Safeguards Technologies at Pacific Northwest National Laboratory. *Procedia Chemistry* **2012**, *7*, 716-724. DOI: 10.1016/j.proche.2012.10.109.
(7) Branch, S. D.; Felmy, H. M.; Schafer Medina, A.; Bryan, S. A.; Lines, A. M. Exploring the Complex Chemistry of Uranium within Molten Chloride Salts. *Industrial & Engineering Chemistry Research* **2023**, *62* (37), 14901-14909. DOI: 10.1021/acs.iecr.3c02005.
(8) Lackey, H. E.; Sell, R. L.; Nelson, G. L.; Bryan, T. A.; Lines, A. M.; Bryan, S. A. Practical Guide to Chemometric Analysis of Optical Spectroscopic Data. *Journal of Chemical Education* **2023**, *100* (7), 2608-2626. DOI: 10.1021/acs.jchemed.2c01112.
(9) Mattio, E.; Caleyron, A.; Miguirditchian, M.; Lines, A. M.; Bryan, S. A.; Lackey, H. E.; Rodriguez-Ruiz, I.; Lamadie, F. Microfluidic In-Situ Spectrophotometric Approaches to Tackle Actinides Analysis in Multiple Oxidation States. *Appl Spectrosc* **2022**, *76* (5), 580-589. DOI: 10.1177/00037028211063916 From NLM Medline.
(10) Felmy, H. M.; Clifford, A. J.; Medina, A. S.; Cox, R. M.; Wilson, J. M.; Lines, A. M.; Bryan, S. A. On-Line Monitoring of Gas-Phase Molecular Iodine Using Raman and Fluorescence Spectroscopy Paired with Chemometric Analysis. *Environ Sci Technol* **2021**, *55* (6), 3898-3908. DOI: 10.1021/acs.est.0c06137 From NLM Medline.
(11) Nelson, G. L.; Lackey, H. E.; Bello, J. M.; Felmy, H. M.; Bryan, H. B.; Lamadie, F.; Bryan, S. A.; Lines, A. M. Enabling Microscale Processing: Combined Raman and Absorbance Spectroscopy for Microfluidic On-Line Monitoring. *Anal Chem* **2021**, *93* (3), 1643-1651. DOI: 10.1021/acs.analchem.0c04225 From NLM PubMed-not-MEDLINE.
(12) Hughey, K. D.; Bradley, A. M.; Tonkyn, R. G.; Felmy, H. M.; Blake, T. A.; Bryan, S. A.; Johnson, T. J.; Lines, A. M. Absolute Band Intensity of the Iodine Monochloride Fundamental Mode for Infrared Sensing and Quantitative Analysis. *The Journal of Physical Chemistry A* **2020**, *124* (46), 9578-9588. DOI: 10.1021/acs.jpca.0c07353 From NLM PubMed-not-MEDLINE.
(13) Lines, A. M.; Bello, J. M.; Gasbarro, C.; Bryan, S. A. Combined Raman and Turbidity Probe for Real-Time Analysis of Variable Turbidity Streams. *Analytical Chemistry* **2022**, *94* (8), 3652-3660. DOI: 10.1021/acs.analchem.1c05228 From NLM Medline.

(14) Cui, Y. *Use Machine Learning to Improve Burnup Measurement in Pebble Bed Reactors*; United States, 2021. https://www.osti.gov/biblio/1822321 https://www.osti.gov/servlets/purl/1822321DOI: 10.2172/1822321.
(15) Felmy, H. M.; Lackey, H. E.; Medina, A. S.; Minette, M. J.; Bryan, S. A.; Lines, A. M. Leveraging Multiple Raman Excitation Wavelength Systems for Process Monitoring of Nuclear Waste Streams. *ACS ES&T Water* **2022**, *2* (3), 465-473. DOI: 10.1021/acsestwater.1c00408.
(16) Lackey, H. E.; Espley, A. F.; Potter, S. M.; Lamadie, F.; Miguirditchian, M.; Nelson, G. L.; Bryan, S. A.; Lines, A. M. Quantification of Lanthanides on a PMMA Microfluidic Device with Three Optical Pathlengths Using PCR of UV–Visible, NIR, and Raman Spectroscopy. *ACS Omega* **2024**, *9* (37), 38548-38556. DOI: 10.1021/acsomega.4c03857.
(17) The MathWorks Inc. (2022). MATLAB version: 9.13.0 (R2022b), Natick, Massachusetts: The MathWorks Inc. https://www.mathworks.com.
(18) PLS_Toolbox 9.2.1 (2023). Eigenvector Research, Inc., Manson, WA USA 98831; software available at http://www.eigenvector.com.
(19) Vigneau, E.; Devaux, M. F.; Qannari, E. M.; Robert, P. Principal component regression, ridge regression and ridge principal component regression in spectroscopy calibration. *J Chemometr* **1997**, *11* (3), 239-249. DOI: https://doi.org/10.1002/(SICI)1099-128X(199705)11:3<239::AID-CEM470>3.0.CO;2-A (acccessed 2025/05/15).
(20) Hult, M.; Andreotti, E.; González de Orduña, R.; Pommé, S.; Yeltepe, E. Quantification of uranium-238 in environmental samples using gamma-ray spectrometry. *EPJ Web of Conferences* **2012**, *24*, 10.1051/epjconf/20122407005.
(21) Choi, H.-D.; Kim, J. Basic characterization of uranium by high-resolution gamma spectroscopy. *Nuclear Engineering and Technology* **2018**, *50* (6), 929-936. DOI: https://doi.org/10.1016/j.net.2018.04.008.
(22) Felmy, H. M.; Bessen, N. P.; Lackey, H. E.; Bryan, S. A.; Lines, A. M. Quantification of Uranium in Complex Acid Media: Understanding Speciation and Mitigating for Band Shifts. *ACS Omega* **2023**, *8* (44), 41696-41707. DOI: 10.1021/acsomega.3c06007.
(23) Nelson, G. L.; Lines, A. M.; Casella, A. J.; Bello, J. M.; Bryan, S. A. Development and testing of a novel micro-Raman probe and application of calibration method for the quantitative analysis of microfluidic nitric acid streams. *Analyst* **2018**, *143* (5), 1188-1196, 10.1039/C7AN01761H. DOI: 10.1039/c7an01761h.
(24) Nguyen, C. T. Verification of the 239Pu content, isotopic composition and age of plutonium in Pu–Be neutron sources by gamma-spectrometry. *Nuclear Instruments and Methods in Physics Research Section B: Beam Interactions with Materials and Atoms* **2006**, *251* (1), 227-236. DOI: https://doi.org/10.1016/j.nimb.2006.06.004.
(25) Lines, A. M.; Adami, S. R.; Sinkov, S. I.; Lumetta, G. J.; Bryan, S. A. Multivariate Analysis for Quantification of Plutonium(IV) in Nitric Acid Based on Absorption Spectra. *Anal Chem* **2017**, *89* (17), 9354-9359. DOI: 10.1021/acs.analchem.7b02161 From NLM PubMed-not-MEDLINE.